High resolution STM analysis of self-assembled monolayers on Au (111)

Maciej Dendzik

Jagiellonian University

Institute of Physics

A thesis submitted for the degree of

Bachelor of Science (B.Sc.)

June, 2011

Składanie oświadczenia obowiązuje od xx/xx 2010 roku.

Wydział Fizyki, Astronomii i Informatyki Stosowanej
Uniwersytet Jagielloński

Oświadczenie

Ja niżej podpisany *Maciej Dendzik* (nr indeksu: 1042847) student Wydziału Fizyki, Astronomii i Informatyki Stosowanej Uniwersytetu Jagiellońskiego kierunku fizyka, oświadczam, że przedłożona przeze mnie praca licencjacka pt. „ *High resolution STM analysis of self – assembled monolayers on Au (111)*'' przedstawia wyniki badań wykonanych przeze mnie osobiście, pod kierunkiem dr hab. *Piotra Cyganika*. Pracę napisałem samodzielnie.

Oświadczam, że moja praca dyplomowa została opracowana zgodnie z Ustawą o prawie autorskim i prawach pokrewnych z dnia 4 lutego 1994 r. (Dziennik Ustaw 1994 nr 24 poz. 83 wraz z późniejszymi zmianami).

Jestem świadom, że niezgodność niniejszego oświadczenia z prawdą ujawniona w dowolnym czasie, niezależnie od skutków prawnych wynikających z ww. ustawy, może spowodować unieważnienie tytułu nabytego na podstawie tej pracy.

Kraków, dnia …… ……

podpis studentki/studenta

Wypełnione i podpisane oświadczenie należy dołączyć do pracy dyplomowej po stronie tytułowej.

2031903654(2)

Contents

1 Preface

But I am not afraid to consider the final question as to whether, ultimately-in the great future-we can arrange the atoms the way we want, the very atoms, all the way down!

- Richard P. Feynman, Nobel Prize in Physics winner, *There's Plenty of Room at the Bottom,* 1958.

The term *Nanotechnology* was coined by Norio Tanaguchi in 1974 as: *Nano-technology mainly consists of the processing of, separation, consolidation, and deformation of materials by one atom or one molecule.* However, probably the first person to see the possibility of designing devices of atomic size was Richard P. Feynman. Charles Kittel in his famous textbook *Introduction to Solid State Physics* defines the term of nanostructure as *a condensed matter structure having a minimum dimension approximately between* $1\,nm$ *and* $10\,nm$*.* Contemporary processors are made in $22\,nm$ technology, so Nanotechnology is present in our daily life. Nanocomposite materials are used widely in medicine or engineering. In molecular electronics a very promising potential applications have Self-Assembled Monolayers (SAMs) which are the topic of this work.

This thesis is a summary of author's research on SAMs on Au(111) surface using Scanning Tunneling Microscopy (STM) during his studies of Physics at Jagiellonian University in Cracow.

First chapter is devoted to essential information about methodology of research. The basic notions and concepts of STM are introduced as well as some of the author's observations. Second chapter is a theoretical introduction to SAM structures that were used in research. In the last chapter, one can find the results of author's research with detailed analysis.

2 Acknowledgments

I would like to thank my supervisor Dr Piotr Cyganik for his time and patience. Special thanks to Prof. Marek Szymoński who guided me through my studies at Jagiellonian University.

3 Introduction to Scanning Tunneling Microscopy

Historical remarks

Probably one of the fundamental objective of solid state physics is to characterize the atomic structure of the sample. It is not an easy task due to some natural limitations of our world. For example diffraction phenomenon limits the resolution of optical microscopy to approximately 0.2 μm. This value makes it practically useless when imaging the objects in the nanometer scale. Such limitation could be later overcame by the application of Electron Microscopy due to short de Broglie wavelength of an electron with the energy in the keV range. Another revolutionary approach to image nanostructures was development of Scanning Probe Microscopy (SPM) which for the first time enabled true three dimensional imaging of the surface. SPM consists of two families of techniques: Atomic Force Microscopy (AFM) and Scanning Tunneling Microscopy (STM). General idea of AFM is to measure the deflection of a cantilever due to atomic forces interaction between tip and the surface. This enables AFM to scan a great variety of samples with high resolution. STM uses quantum effect of electron tunneling to obtain information about topography of a sample. This method limits STM application to conducting or semiconducting samples, but offers the highest resolution. First STM was constructed by Gerd Binnig and Heinrich Rohrer in 1982. For this achievement they were awarded the Nobel Prize in Physics in 1986.

Theory of STM

The basic idea of the STM is shown in Figure 1. A sharp conducting tip is brought close to surface. At the distance of couple of angstroms electrons can tunnel between the tip and the sample through the energy barrier defined by the respective work functions (Figure 1C).

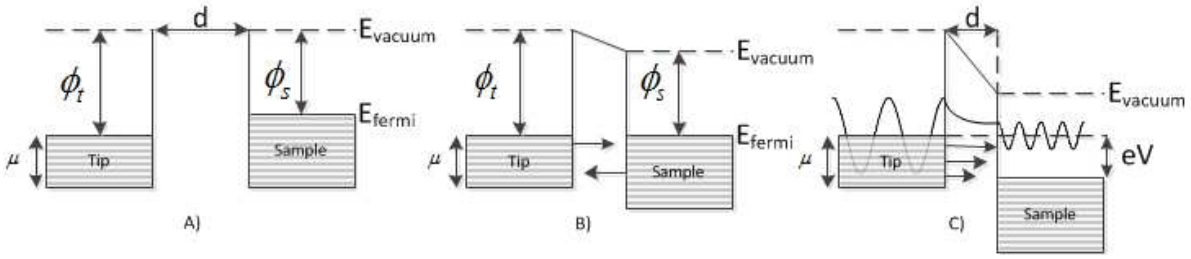

Figure 1 Energy levels diagrams of the tip and the sample. φ - work function , μ - chemical potential, d - distance. A) For distant tip and sample there is no interaction and vacuum levels are equal. B) For tip close to the sample we have connected system with equal Fermi levels. Electrons can tunnel in both directions by swapping places, but the net current is zero C) By applying bias voltage V between the tip and the sample, respective Fermi levels are shifted by the energy eV, and it is possible

for electrons to flow from occupied states to the unoccupied states. The direction of tunneling depends on the voltage polarization.

Physical quantity used for scanning the surface is tunneling current I, so it is crucial to evaluate how does it depend on the distance d between the tip and the sample. For simplicity we can assume that we are dealing with electron tunneling through the square potential barrier of height U. The wave function of the tunneling electron could be written as follows:

$$\psi(d) = \psi(0)\, e^{-\kappa d} \tag{1}$$

where $\kappa = \frac{\sqrt{2mU}}{\hbar}$ and m is the electron mass. In contrary to classical mechanics, there is a nonzero probability $p \sim |\psi(0)|^2 e^{-2\kappa d}$ of finding electron behind the barrier region. For elastic process the energy of an electron does not change after tunneling, so in case of equal Fermi levels the electrons from tip and sample can only swap places and no net current flows. Applying bias voltage V shifts Fermi levels by $eV \ll \varphi$, so the electron from the tip with energy $E_n \in [E_F - eV, E_F]$ has a nonzero probability p of tunneling to the sample (with $\kappa = \frac{\sqrt{2m\varphi}}{\hbar}$). If we assume that the condition of the tip does not change in time during scanning we can conclude that tunneling current is proportional to the number of states on the sample in the energy interval $[E_F - eV, E_F]$.

$$I \sim \sum_{E_F - eV}^{E_F} |\psi_n(0)|^2 e^{-2\kappa d} \tag{2}$$

The continuity of I for atomic scale barriers is a consequence of the uncertainty principle [1]. Equation (2) could be written in a more elegant form using the local density of states at the Fermi level $\rho_S(x, E) \equiv \frac{1}{\varepsilon} \sum_{E-\varepsilon}^{E} |\psi_n(x)|^2$:

$$I \sim V \rho_S(0, E_F)\, e^{-2\kappa d} \tag{3}$$

Considering typical value of the work function for metals ($\varphi \approx 4eV$), the tunneling current decays about 7.4 times per 0.1 nm [1]. This effect makes the STM extremely sensitive to changes of the tip-sample distance, and in consequence enables, as explained in more details below, high resolution surface imaging.

The more advanced model of a metal-insulator-metal (MIM) junction tunneling was established by Bardeen in 1960 [1] and later corrected by Herring in 1962 forming so called modified Bardeen approach (MBA), [2]. General idea of MBA is to consider the subsystems of tip and sample separately and for both solve stationary Schrödinger equation. The rate of electron tunneling is

obtained by application of time-independent perturbation calculation and Fermi golden rule. As a result of this approach the tunneling current I is given by:

$$I = \frac{4\pi e}{\hbar} \int_{-\infty}^{\infty} \left[f\left(E_F - eV + \varepsilon\right) - f\left(E_F + \varepsilon\right) \right] \rho_S \left(E_F - eV + \varepsilon\right) \rho_T \left(E_F + \varepsilon\right) |M|^2 \, d\varepsilon \qquad (4)$$

where $f\left(E\right) = \left(1 + e^{\frac{\left(E - E_F\right)}{k_B T}}\right)^{-1}$ is Fermi distribution and M is tunneling matrix. For evaluating M the shape of the tip is needed. It could be modeled by a hemisphere as shown in Figure 2. The angle dependency is often neglected and calculations are made only for tips s-wave function [3], however this model often fails while estimating atomic resolution of STM and more sophisticated model is needed.

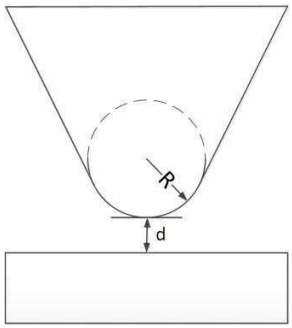

Figure 2 The s-wave-tip model. The effect of a tip's shape was modeled as a potential well with radius R and tip-sample distance R+d [3].

Apart from MBA there are also other approaches for modeling the STM. Extensive discussion about other concepts can be found in [4].

The process of tunneling electrons from sample to the tip is also influenced by the chemical composition of both sample and tip, the electronic structure, and the chemical interactions of both systems. Order of importance of those effects depends on the tip-sample distance and should be treated with care. For example, computer simulations shows that for distances smaller than 0.4-0.5nm chemical forces have profound effect on the tunneling current [5]. Just before the contact at the distance of approximately 0.3nm the tunneling barrier height is rapidly decreasing [6]. It is connected with ions moving back and forth from tip to the sample and some chemical bond are formation. In region of chemical interaction tunneling current increases rapidly and the surface is modified by the tip. Those modifications could be temporary as well as permanent. Moreover, very high electric field density in the neighborhood of the tip can also modify the surface.

Practical realization

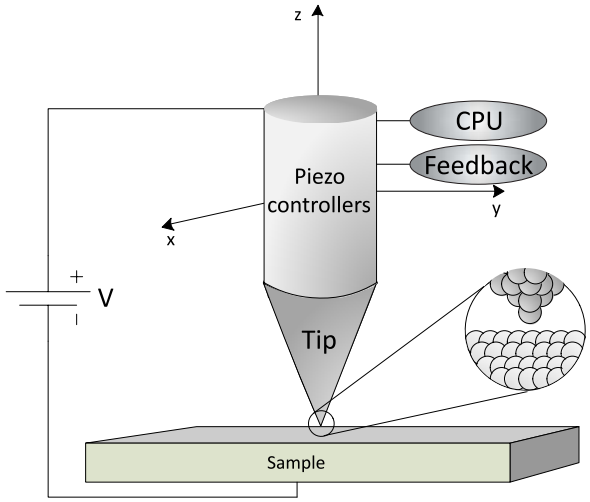

Figure 3 Schematic of STM construction.

Figure 3 shows a simple scheme of the STM. The bias voltage applied between the sample and the tip that enables electrons tunneling through the gap of approx. $\sim 1nm$ width. The lateral and vertical movement of the tip is realized by the precise piezoelectric scanner. The scanning of the tip over the sample surface is possible thanks to the feedback loop system which controls tip-sample distance according to the instantaneous tunneling current value. The feedback loop system is controlled by changing gain parameters i.e. so called proportional and integral gain (Figure 4). The values of gain depend on the sample and could be found experimentally.

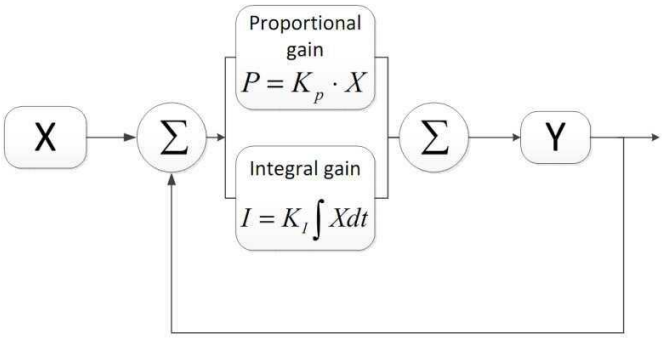

Figure 4 Feeback system used in STM.

The STM can be operated in two basic modes. The most common is so called "constant current" mode. In this mode the tip-sample distance is modified during scanning by the scanner to keep the tunneling current at the constant value defined by the operator. This prevents the tip from crashing into a surface during scanning and at the same time creates image which is reflecting mainly topography of the surface. However, it should be noted at this point that the STM image is in fact always the convolution of the topography and the local electronic structure. For very flat surfaces one can keep the tip-sample distance at fixed value, with the feedback loop system off, and measure the tunneling current while scanning. This mode of operation is called "constant height" mode and allows higher speed of scanning which can be useful while dealing with temperature drift. Importantly, unlike the electron microscope, the STM can also operate out of the vacuum system in ambient atmosphere or even in liquid. The STM can also be used for Scanning Tunneling Spectroscopy (STS) and for modification of the surface, but those topics are beyond the scope of this thesis.

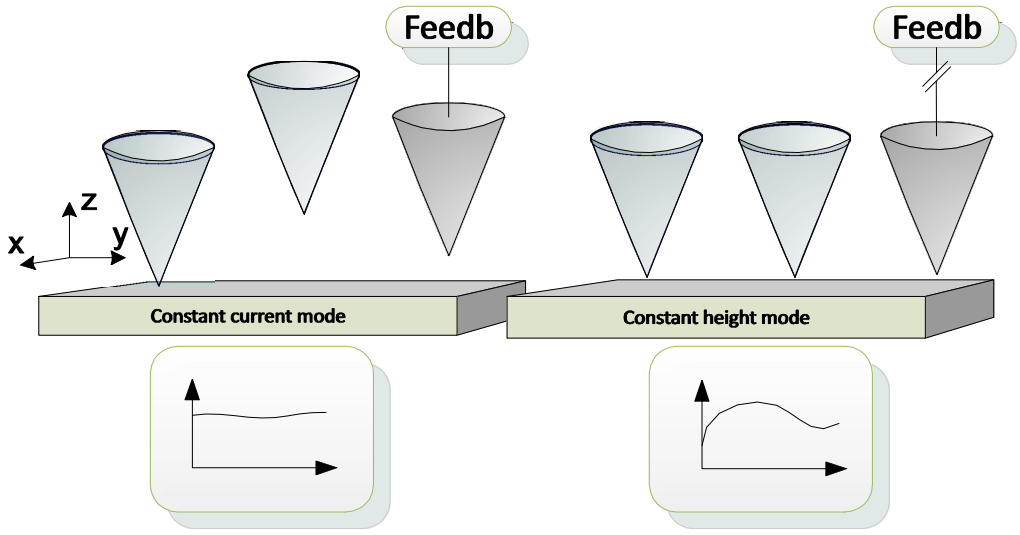

Figure 5 Schematic representation of constant current mode and constant height mode scanning.

A very important aspect of the STM imaging is a proper isolation from the external environment. Due to exponential dependence of the tunneling current on the tip-sample gap even small vibrations can affect the results. For vibration isolation the microscope is placed on active or passive anti-vibration system. In modern research centers, rooms for STM microscopes are specially designed

to be isolated from the rest of the building structure in order to obtain the best possible anti-vibration performance. In the first successful demonstration of vacuum tunneling by Binnig in 1982 vibration isolation was provided by magnetic levitation using superconductors working at liquid helium temperature [7]. Apart from pure mechanical disturbances electro-magnetic field can also distort the images. During author's research some Faraday's cage appliance was used in order to minimalize this effect. Thermal drift is another important issue for high-resolution STM. The temperature of the laboratory should be kept constant during scanning and system should be left for sufficient amount of time in order to reach the thermal equilibrium.

Considering now the drawbacks of the STM beyond the obvious one, it is the limitation of this technique to the conductive samples, it should be noted that the predominant influence on the STM image quality has the shape and chemical composition of the STM tip apex. Although, there are several methods of STM tip preparation which allow controlling tip shape and chemical composition, the tip apex is modified also while scanning. This problem is particularly visible for experiments conducted in ambient conditions. To solve this problem one can try intentionally modify the tip during scanning to change its apex back to the conditions at which high resolution images are obtained. For example it can be realized during the scanning by significant change of the bias voltage (by several volts) for a short period of time. This causes a very strong interaction between the tip and sample and leads to the tip apex modification). Another method is to fiddle with the scanning speed and the image size.

As far as image processing is considered, there are two important steps in this process. First usual step is so called "flattening". This is just a method of subtracting the globally or locally tilting of the image plane by averaging the neighboring points of the image. Typically, we can choose the order of polynomial which will be subtracted or point the set of points from which the average will be calculated. If there is some defect visible on the image we can exclude it from flattening. In the next step for denoising image the Fast Fourier Transform (FFT) can be applied followed by specific frequency filtering .

4 Self-Assembled Monolayers (SAMs)

SAMs in Nanotechnology

The most obvious difference between macroscopic materials and nanometer scale structures is the percentage of constituent atoms laying on the surface. Due to different scaling of the volume and area with the dimensions x of the structure $(\frac{S}{V} \sim \frac{1}{x})$ nanostructures have high percentage of the surface atoms. The greatest gradients in properties are present on the interface making characteristics of nanostructures different than bulk materials. Using this fact we can tailor the interfacial properties of metals and semiconductors by coating the surface with suitable covering. Self-Assembled Monolayers (SAMs) provide a simple, flexible and cheap way to realize this task. Using such a modification we can control hydrophobicity, friction, adhesion or wear of a substrate.

SAMs can be defined as the organic assemblies which form quasi-two-dimensional structures formed by the absorption from solution or the gas phase onto the substrate. The process of SAMs formation is spontaneous and leads to organization into stable, crystalline structures with alterable chemical functionality at the exposed interface. Thickness of SAM is well defined $1 - 3nm$ and can act as a physical barrier. Thus, SAMs form natural 2D nanostructures. Due to absorption of SAM electronic properties of the substrate are changed. Moreover, SAMs can be used as organometallic junctions enabling organic structures to be joint to metal surface. The fact that process of SAMs preparation does not require ultrahigh vacuum conditions or specialized equipment together with their unique properties makes SAMs a subject of intensive studies in nanotechnology.

Structure of SAMs

Typical SAM molecule consist of three building blocks which are schematically shown in Figure 6. The part of molecule which binds to a surface is called head group. This group is responsible for chemical bonding of the SAM forming molecule to the substrate. Due to the exothermic head group-substrate reaction the adsorption process of SAMs is spontaneous. Head groups are connected to terminal groups with the spacer chains. Interaction between neighboring spacer chains is of Van der Waals type. The energy of such an interaction depends on the length of the SAM forming molecule its chemical composition and packing density in the monolayer. For instance in the case of hexadecanethiol SAMs, which are the most popular, the intermolecular interaction of the given molecule with their closest neighbors in the monolayer was estimated to 1.1 eV. SAMs molecules are usually not normal to the surface, but tilted by the angle α as shown schematically in Figure 6. The value of this angle depends on the spacer chain, head groups and substrate used. For example in hexadecanethiol SAMs on Au(111) substrate $\alpha \approx 35°$.

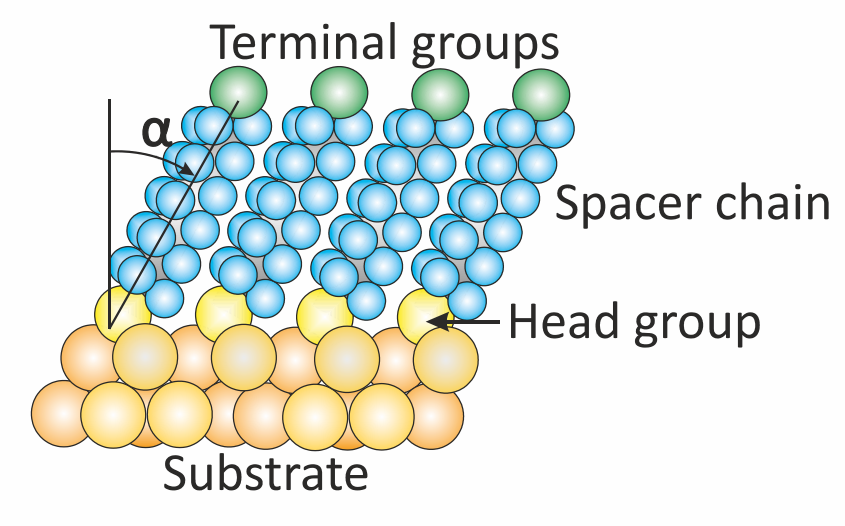

Figure 6 Schematic representation of SAM molecules on the metal substrate.

The most usual method of SAMs formation is incubation of the substrate in solution containing precursor molecules which can react chemically with the substrate surface. The other method is to expose the substrate to a vapor of the reactive molecules. The typical precursors and respective substrates used for SAMs formation are listed in Figure 7. The most important among them are thiols, carboxyls and silanes which enables formation of SAMs on metal (Au, Ag, Cu, Ni), semiconductor (GaAs, Si) or isolator (mica, glass) substrate.

Substrate	Precursor	Binding with substrate
Au	RSH (thiol)	RS-Au
Au	ArSH (thiol)	ArS-Au
Au	RSSR (disulfide)	RS-Au
Au	RSR (sulfide)	RS-Au
Si/SiO_2	$RSiCl_3$ (trichlorosilane)	Si-O-Si (Siloxane)
Si/Si-H	RCOOH (carboxyl)	R-Si
Metal Oxides	RCOOH (carboxyl)	RCOO-... MO_n

Figure 7 The most commonly used substrates and precursors for SAM formation [8]**.** R**represents alkane** (C_nH_{2n+2}) **and** Ar **aromatic hudrocarbon.**

Thiol and Selenol based SAMs on Au(111) substrate

Thiols due to high stability and low costs are the most common precursors in SAM formation. During last 30 years SAMs based on thiols have been a subject of intensive studies analyzing their

structure and properties [9]. As it is well documented by recent review [9] the range of thiol based SAMs applications is so wide that it can be treated as separate branch in nanotechnology research.

The idea to use selenols is relatively new and not yet studied enough, but they tend to have similar properties. Selenols form better organized structures with lower number of defects. Those properties are crucial in terms of molecular electronics application. Moreover, binding Se-Au(111) is stronger than S-Au(111) with less corrugated energy hypersurface (see Figure 8). For this reason Se atoms have higher mobility on the surface and at the same time make more stable binding [11]. Finally, it is highly probable that selenols have better electric conductivity than their thiol analogues. All of those features make selenols an interesting target of further SAMs research.

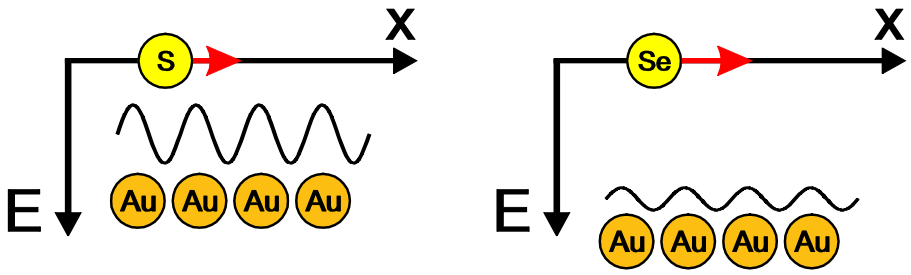

Figure 8 Schematic represantation of differences between bondings S-Au(111) and Se-Au(111). Red arrows represents the surface mobility of Se and S atoms. More comment in the text above.

For dilute solutions of thiols or selenols on Au(111) the process of SAMs formation consist of two steps. In the first step, which lasts couple of minutes, head groups of SAMs precursors binds chemically to the surface. The energy of this chemical binding for thiols is estimated for $\sim 1.6 - 2eV/molecule$. For selenols binding energy to the Au(111) substrate is expected to be larger however quantitative approximation of the binding energy is yet not available. Kinetic studies shows that 80-90% of the maximal film thickness is reached during the first step. Also contact angles measured during this step reach close values to the final ones. The first step lasts longer for more diluted solutions i.e. for $1mM$ it requires ~ 1 min and for $1\mu M$ more than 100 min. The second step consist of the final self-organization of the SAMs crystalline structure and last couple of hours and after that fully developed structure is formed. The organization process during the second step is driven by the Van der Waals interactions between the spacer chains. Kinetics of this step is faster for longer alkyl chains. The kinetics of SAMs adsorption during the first step usually can be relatively good approximated by the simple Langmuir process, however, for molecules with significant intermolecular interactions (eg. significant permanent dipole moment), which are not included in Langmuir model, such approach is insufficient.

Practical applications of SAMs

One of the reasons of large interest in SAMs is the fact that they enables us to study the contribution of molecular composition to macroscopic properties. SAMs are prototypes of nanotechnology by means of generating organized structure without any further influence. Great variety of usable molecules contribute to wide application in the fields of molecular electronics, lithography, biotechnology or tribology. Couple of interesting applications can be found in this section.

SAMs are used in the OLED (Organic Light Emitting Diode) and OFET (Organic Field Emission Transistor) devices for changing the energy differences between the Fermi level in metal and HOMO (Highest Occupied Molecular Orbital) for the holes and LUMO (Lowest Unoccupied Molecular Orbital) for electrons in organic semiconductor. Such a solution increases the efficiency of OLED and OFET devices. Non-conducting SAMs can be used as an isolator for gate electrode in OFETs.

Another interesting application of SAMs in the field of molecular electronics is their usage as the memory devices and switches. The first successful attempt was to use STM tip for initiating the conductance switching phenomenon for isolated molecules in SAMs. This approach lacks of potential commercial realization and was replaced by the more practical methods such as light triggering mechanism. For instance it was shown [12] that after exposing specially designed SAMs to the light of specific wavelength the major change of conductivity is observed. However, we should note at this point that the most promising solution for molecular memories is to use voltage pulses both for reading, writing and erasing data. Such possibility was demonstrated using aromatic SAMs with NO_2 side groups. Molecular memories created by them enables achieving resistance ratio for on\off states of ~ 370 with exponential retention time constant of ~ 69 s [13].

In lithographical applications SAMs can be used not only as a mask for chemical etching, but also for selective absorption of other materials. DPN (Dip Pen Nanolithography) uses AFM tip immersed in the solution of precursors to grow the SAMs on the specific areas with the resolution of couple nanometers. This technique enables to manufacture nanosensors with biological components [14].

For designing NEMS (Nanoelectromechanical structure) tribological parameters such as friction, adhesion or wettability play a major role. By coating the surface with appropriate SAMs one can tailor those parameters for specific tasks, making NEMS more effective. The impact of SAMs on the coefficient of friction is shown in the Figure 9.

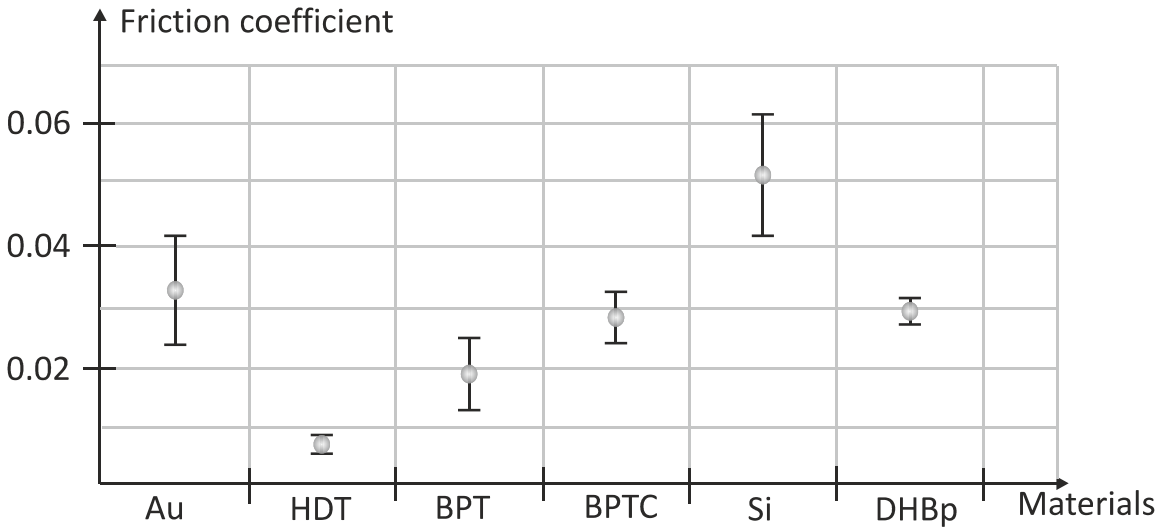

Figure 9 Changes of the friction coefficient due to different SAMs coating. On Au substrate: HDT- Hexadecanethiol, BPT- biphenylthiol, BPTC- cross-linked biphenylthiol. On Si substate: DHBp- dihydroxylbiphenyl [8].

Presented above examples are only a small fraction of today's potential SAMs applications. For most of them the main obstacle is the level of SAMs structural perfection. In order to use SAMs for large, commercial applications the methodology of their formation should be improved to reduce defects concentration. To achieve this goal more must be known about the process of SAMs formation to increase our control of this process. The aim of author's project was to investigate some aspects of this interesting phenomenon.

5 Temperature induced modification of the BPnSe SAM structure on Au(111)

Thiol based SAMs have been extensively studied during last years and its ability to form organized structures on the surface is indisputable. Due to similar physical properties of selen and sulfur it is reasonable to expect the same behavior of selenol based SAMs. This section focuses on the selenol based SAMs on Au(111) surface, their structure and coverage of the substrate.

It was shown in [15] that BPnSe SAMs form organized structures on Au(111) surface. Similarly as their thiol analogues BPnSe exhibit different structure depending on the parity of parameter n which defines the length of alkane chain (see Figure 10). Odd numbered BPnSe/Au(111) have $\left(2\sqrt{3}\times\sqrt{3}\right)R30^{\circ}$ structure with two molecules per unit cell and area per molecule of $0.216\,nm^2$. For even numbered BPnSe/Au(111) surface structure can be described by anisotropic expansion of

the above structure along the shorter cell vector which results in area per molecule in the range of $0.260 - 0.275\,nm^2$. From this we can conclude that such an effect is general property for aliphatic SAMs with chalcogen headgroups. More about odd-even effect can be found in [11] and [15].

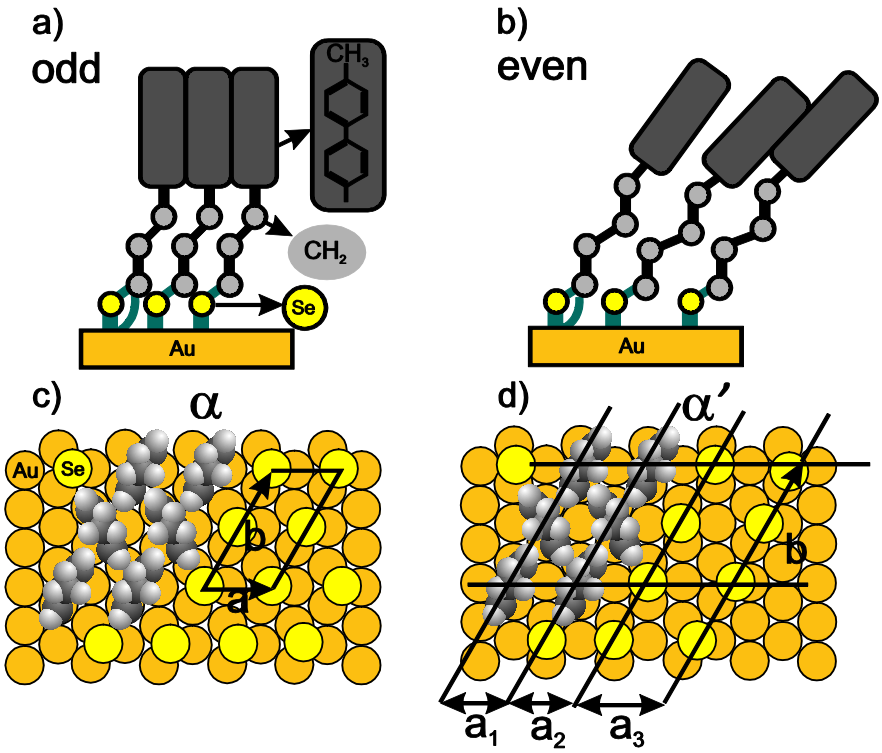

Figure 10 Schematic representation of the odd-even effect for BPnSe SAMs with phases α and α'. (a-b) side views of the structures with odd and even number n with tilted phenyl rings. The $\left(2\sqrt{3}\times\sqrt{3}\right)R30°$unit is marked with vectors a and b in a). The same structure expanded along direction vector a in b).

Previous research of BPnS/Au(111), which are thiol analogues of BPnSe/Au(111), showed that new structure phases of these SAMs can be observed when prepared at elevated temperatures. Importantly, these new phases were characterized by higher stability and lower defect density[15]. Considering similar odd-even effects in structure and stability of BPnSe/Au(111) and BPnS/Au(111) it is reasonable to expect formation of new phases in the case of BPnSe/Au(111) SAMs. Following this expectation, the topic of my research focused on structure analysis, by means of STM, of BPnSe/Au(111) SAMs prepared at elevated temperature.

Experimental setup

Molecules used in experiments were diselenide compounds
($BPnSe-SeBPn: CH_3\,(C_6H_4)_2\,Se-Se\,(CH_2)_n\,(C_6H_4)_2\,CH_3$) (n = 1-6). All molecules were synthesized by Prof. Terfort group at Frankfurt University. The gold films were prepared in evaporation chamber at 610 K by evaporating approx. 150 nm of gold on mica substrate. In order to remove residual water mica substrate had been heated and stored for 24 h under vacuum conditions before deposition process. After deposition, samples were flame-annealed with butane/oxygen flame. The following procedure resulted in high-quality Au(111) films with large terraces and step faceting along $\langle 1\bar{1}0\rangle$ directions. SAMs were prepared by immersing substrate into 0.1 mM solution of BPnSe in ethanol. This process was conducted in several different temperatures, ambient conditions and for different amount of time. In final treatment samples were rinsed in ethanol and blown dry with nitrogen

STM measurements were done using MultiMode IIIa (Digital Instruments) microscope at room temperature in air environment. Tips were manufactured mechanically by cutting a 0.25 mm wire made of Pt/Ir alloy (8:2, Goodfellow). Constant current mode was used for data acquisition.

Structure of BPnSe/Au(111) SAMs formed at elevated temperatures

BPnSe/Au(111) with even value of n. Conducted research with BPnSe/Au(111) prepared at the higher temperature ($60^{\circ}C$) clearly shows new structural phases for molecules with even number n. Apart from α phase which was present in the samples prepared at room temperature, two new phases were observed which are denoted here by β and γ. For BP4Se/Au(111) these new phases were coexisting with phase α as documented by the data shown in the Figure 11a. High-resolution data in Figure 11b and Figure 11c show structure of new phases in more details. To analyze these new structures corresponding height profiles are presented in Figures 11(d-g). Basing on these STM data we propose structural models corresponding to phases β and γ as schematically presented in Figure 13. For phase β and γ structure $\left(2\sqrt{3}\times 5\right)$ with $a = 1.48\,(0.09)\ nm$ and $b = 1.42\,(0.07)\ nm$ and $\left(2\sqrt{3}\times 6\sqrt{3}\right)$ with $a = 1.15\,(0.11)\ nm$ and $b = 3.11\,(0.17)\ nm$ were assumed, respectively. The area per molecule corresponding to these structures are $0.36\,nm^2$for β and $0.25\,nm^2$ for γ.

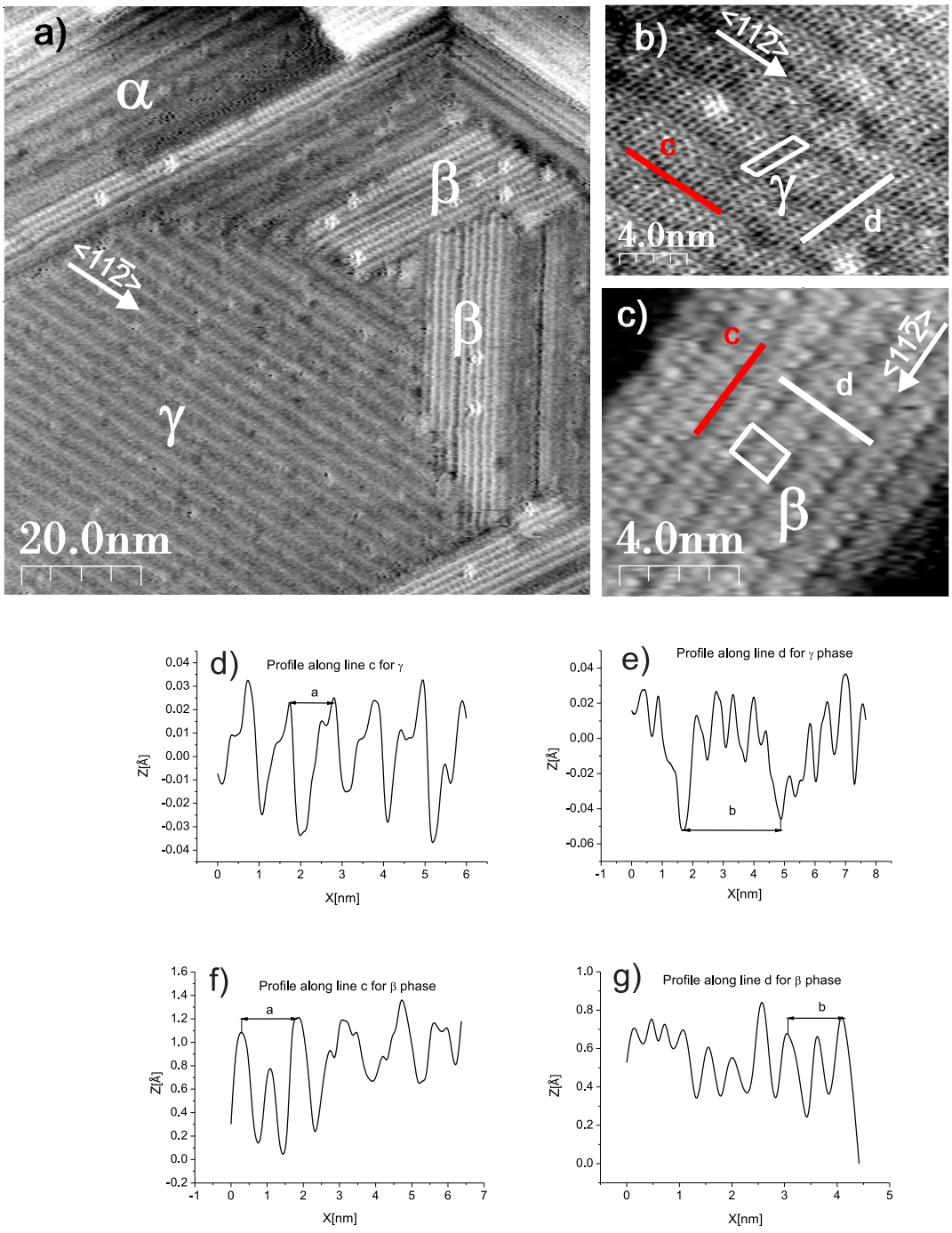

Figure 11. (a-c) STM data for BP4Se/Au(111) prepared at the temperature $65°C$ (24h of incubation) showing coexistence of α, β, γ phases. (f-g) Height profiles for γ and β phases along lines marked in (a-c).

1693546894(18)

The corresponding STM data obtained for BP2Se/Au(111) are presented in Figure 12. In this case only one new phase was observed. The height profiles presented in Figure 12 indicate that rectangular unit cell of these new phase has dimensions $a = 1.51\,(0.06)\ nm$ and $b = 1.50\,(0.07)\ nm$ which are corresponding to phase β described above for BP4Se/Au(111).

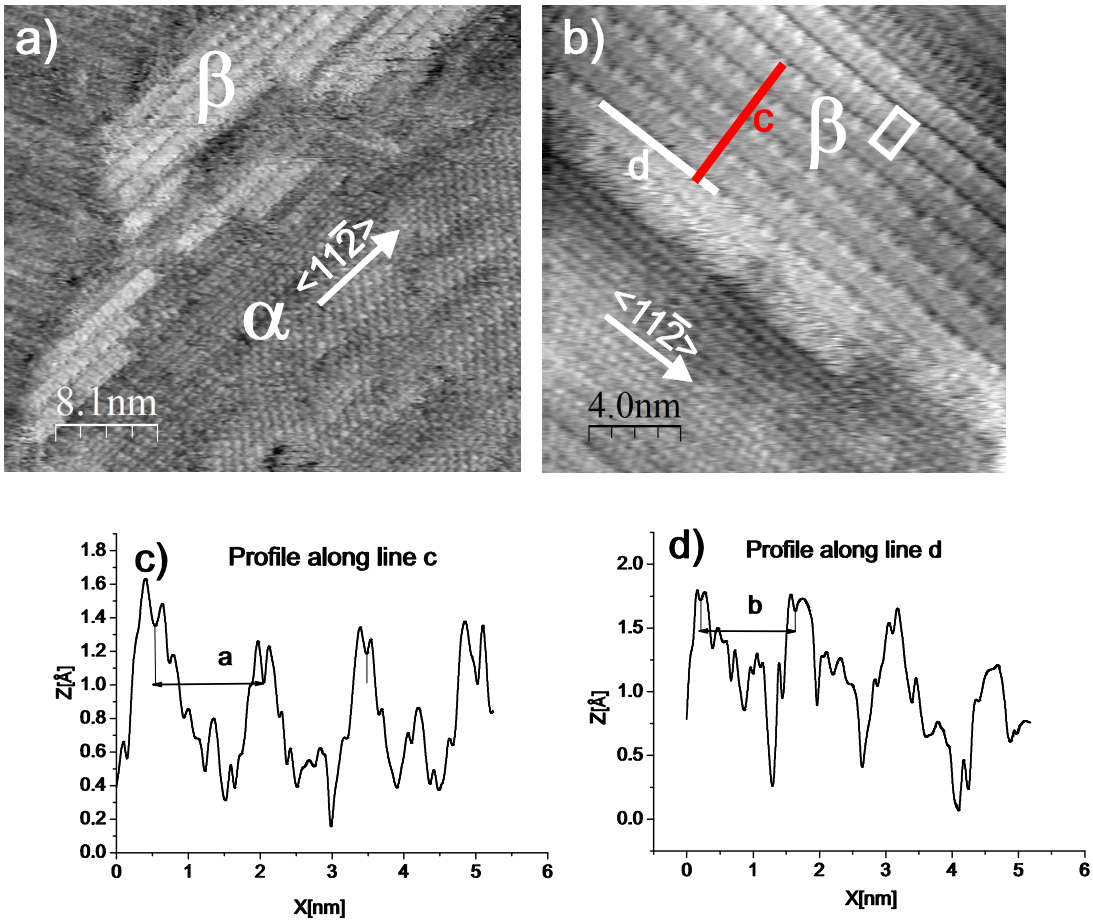

Figure 12 (a-b) α, β phases in the STM data of the BP2Se/Au(111) prepared at the temperature $65°C$ (24h of incubation). (c-d) Profiles showing topography along lines marked in b).

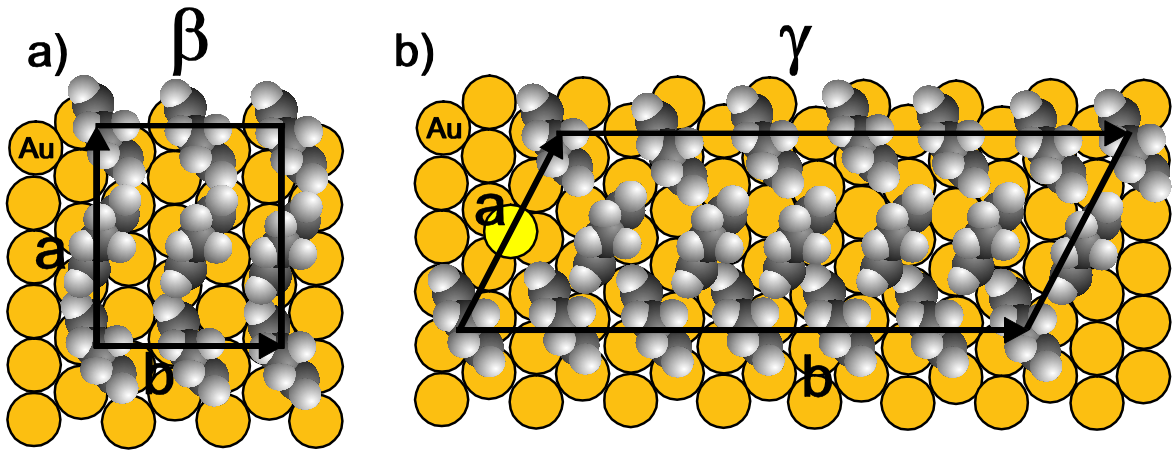

Figure 13 a) Proposed schematic of the β phase unit cell with rectangular $\left(2\sqrt{3}\times 5\right)$ structure on Au(111). b) Proposed schematic structure of the γ phase with oblique $\left(2\sqrt{3}\times 6\sqrt{3}\right)$ unit cell on Au(111).

BPnSe/Au(111) with odd n. STM data obtained for BP3Se/Au(111) and BP5Se/Au(111) prepared at the higher temperature ($60°C$) are presented in Figure 14 Figure 15, respectively. For both SAMs only one oblique structure was observed. The analysis of unit cell vectors of this structure for BP3Se/Au(111) from corresponding height profiles delivers values of $a = 0.58\,(0.09)\,nm$ and $b = 0.91\,(0.06)\,nm$. Corresponding values obtained for BP5Se were very similar i.e. $a = 0.52(0.9)\,nm$, $b = 1.01(0.09)\,nm$. This structure can be identified as structure α which was reported previously for odd BPnSe/Au(111) structures prepared at room temperature (see Figure 10).

4862051606(20)

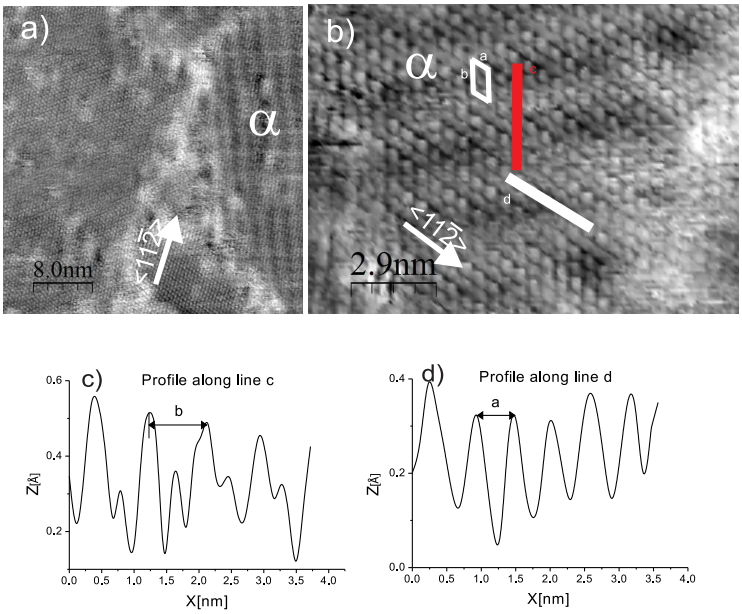

Figure 14. (a-b) STM data for the BP3Se/Au(111) prepared at the temperature $65°C$ (24h of incubation). (c-d) Profiles below STM images show topography along lines marked in b).

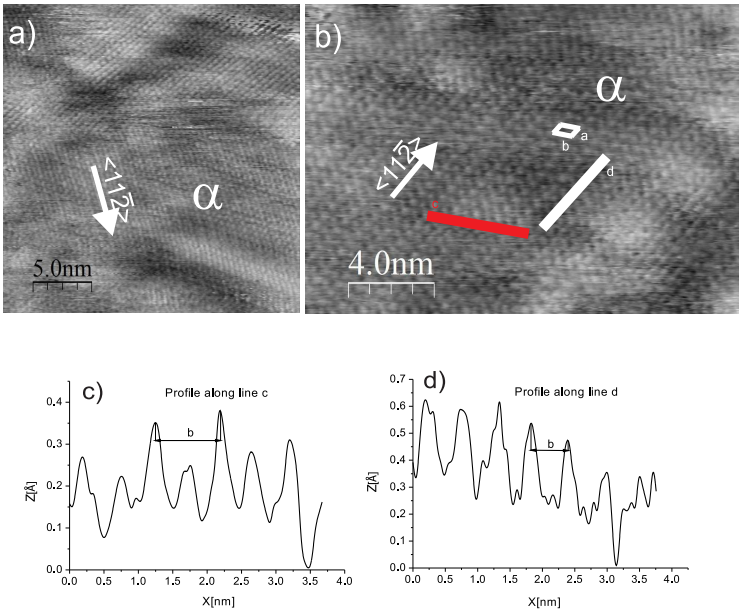

Figure 15 (a-b) STM data for the BP5Se/Au(111) prepared at the temperature $65°C$ (24h of incubation). (c-d) Height profiles along lines c and d marked in b).

Coverage calculation of the β phase for even numbered BPnSe/Au(111).

New phase β is clearly visible on the large scale STM images (see Figure 16). Such images were used for approximation of the β phase coverage for even numbered BPnSe/Au(111).

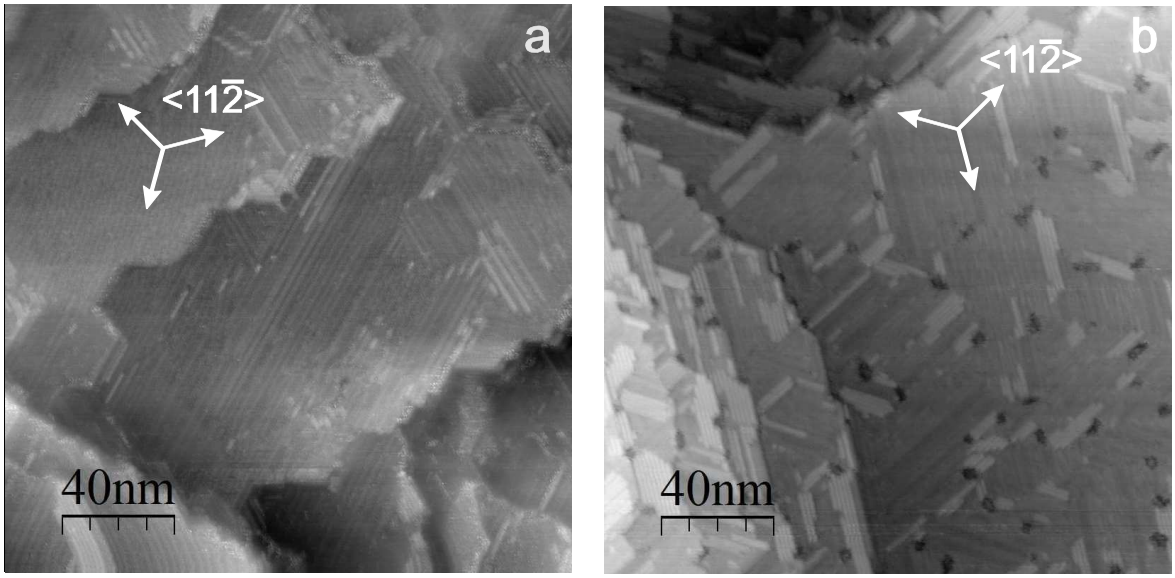

Figure 16 STM images of the a) BP4Se b) BP2Se SAMs on Au(111).

β phase domains formed on the surface have typical size of $100 - 1200\,nm^2$. Color histograms of the STM images were analyzed in order to estimate the area of a domain. Analysis of the color histograms show that for the image in grey scale (0-255) there is no white color (255) and therefore this color was chosen to mark interesting area of the image. From histogram of processed image the area of the domains was calculated. Sample coverage was estimated after analysis of couple 250nm x 250nm images. The procedure of area calculations is depicted in Figure 17. This analysis revealed that for BP2SeAu/(111) the coverage of β phase is approx. 20%. Due to lower contrast quality for large scale images corresponding analysis was not possible for BP4Se/Au(111).

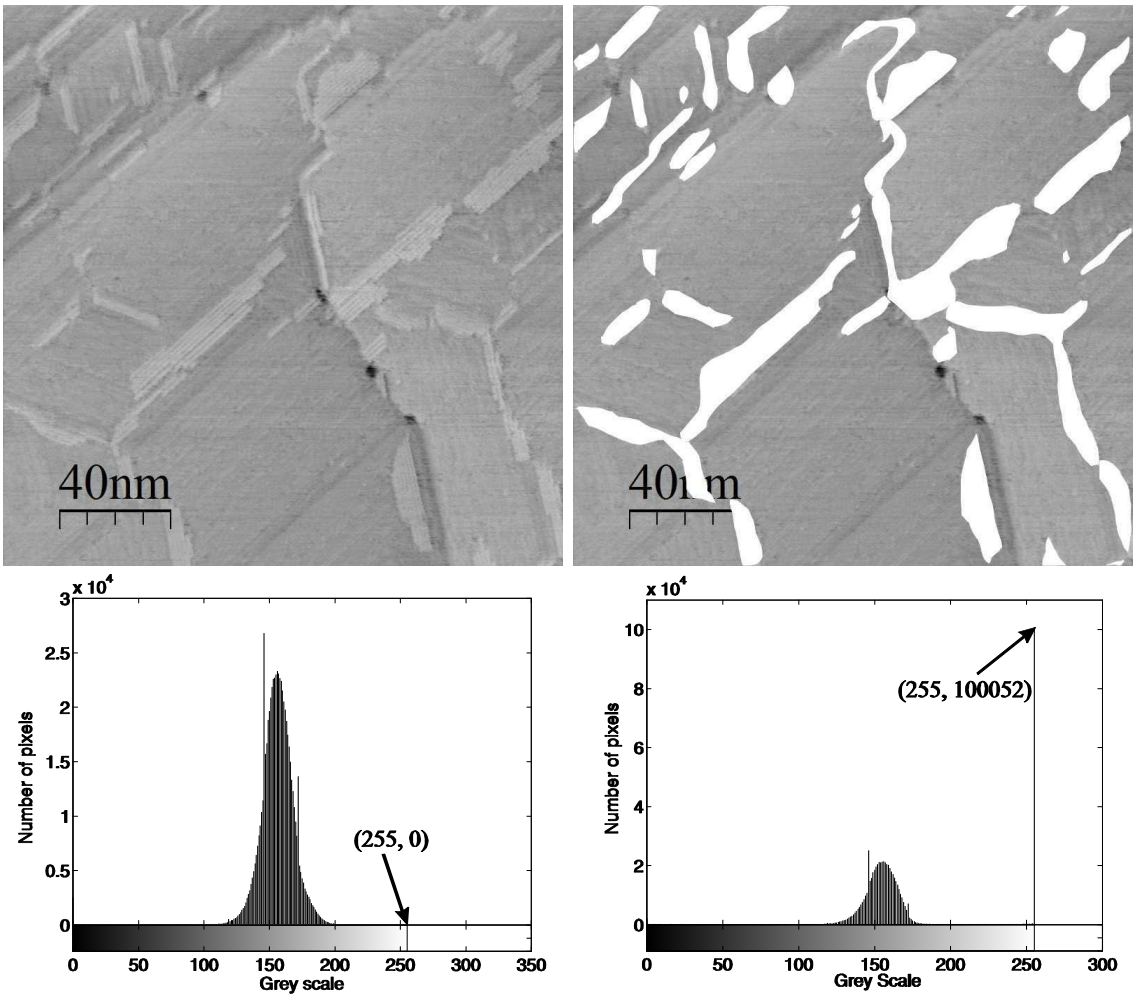

Figure 17 STM images of the BP2Se/Au(111) with corresponding histograms. Image on the right shows marked domains of SAM with visible peak at white color (255).

In order to obtain full transition to one of the new phases BP4Se/Au(111) samples were prepared at different temperatures of the solution (in the range of $50-80°C$) and incubation time ($6-120h$). In all cases, however, no significant increase of the coverage was observed. Instead, at temperatures above $70°C$ destruction of the monolayer structure was observed (see Figure 18).

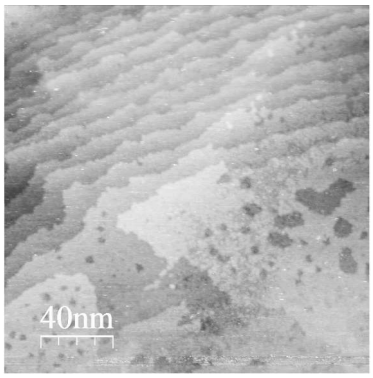

Figure 18 BP4Se/Au(111) prepared in solution at $80°C$.

Summary and discussion

BPnSe/Au(111) SAMs tends to form significantly larger domains comparing to BPnS/Au(111. For selenols domains have approx. 30-80nm in diameter, whereas for thiols this value was 5-20nm for the same preparation conditions.

Molecular structure of BPnSe/Au(111) SAMs with n=2-6 prepared at room temperature shows similar structure to $\left(2\sqrt{3}\times\sqrt{3}\right)R30°$ with two molecules per unit cell as shown in Figure 10. For BPnSe with odd value of parameter n we can observe better organization and regular values of both a and b unit cell vectors. For systems with even value of parameter n observed structure can be described as irregular expansion of $\left(2\sqrt{3}\times\sqrt{3}\right)R30°$ structure along its shorter unit vector (vector$a$). Due to this irregularities, such systems have 22-28% lower packing density than their odd numbered analogues.

Increasing temperature during BPnSe/Au(111) SAMs formation leads to new phases creation. However, this process is observed only for systems with even value of parameter n. This phenomenon could be explained by lower stability of the even numbered BPnSe which makes them more prone to structural changes at the elevated temperatures. In this sense BPnSe/Au(111) SAMs are very similar to their thiol analogs for which same phenomenon was observed i.e. new phases formation for even numbered BPnS/Au(111) SAMs [16]. However, formation of these new phases for BPnS/Au(111), was observed at higher temperature of the solution. The reason for this difference could be related to different bonding of sulfur and selenium on Au(111) surface. As proposed in [15] in case of BPnSe/Au(111) binding energy hypersurface is less corrugated as compared to BPnS/Au(111) making molecules in BPnSe/Au(111) SAMs more mobile on the Au(111) surface (see Figure 9). Therefore, less energy is needed for SAM structure to get into new phase.

Reference

[1] Chen,C. J., *Introduction to Scanning Tunneling Miscoscopy*, Oxford Science Publications 1993.

[2] Bardeen,J. , *Phys. Rev. Lett.* 1961, *6*, 57–59.

[3] Tersoff,J. , Hamann,D. R., , American Physical Society 1985, p.p. 805–813.

[4] D Drakova, *Reports on Progress in Physics* 2001, *64*, 205.

[5] Bowker,M. , Davies,P. R., , Wiley-VCH Verlag GmbH 2010, p.p. 98-99.

[6] Gimzewski,J. K., Moller,R. , , American Physical Society 1987, p.p. 1284–1287.

[7] Binnig,G. , Rohrer,H. , Gerber,C. , Weibel,E. , , *Applied Physics Letters* 1982, *40*, 178-180.

[8] Bharat Bhusha, *Springer Hanbook of Nanotechnology*, Springer 2004.

[9] Love,J. , Estroff,L. , Kriebel,J. , Nuzzo,R. , Whitesides,G. , *Chemical Reviews* 2005, *105*, 1103-1169.

[10] Ulman,A. , *Chemical Review* 1996, *96*, 1533-1554.

[11] Szelagowska-Kunstman,K. , Cyganik,P. , Schuepbach,B. , Terfort,A. , *Physical Chemistry Chemical Physics* 2010, *12*, 4400-4406.

[12] Kronemeijer,A. J., Akkerman,H. B., Kudernac,T. , van Wees,B. J., *et al.*, *Advanced Materials* 2008, *20*, 1467+.

[13] Li,C. , Zhang,D. , Liu,X. , Han,S. , *et al.*, *Applied physics letters* 2003, *82*, 645-647.

[14] Lee,K. , Park,S. , Mirkin,C. , Smith,J. , Mrksich,M. , *Science* 2002, *295*, 1702-1705.

[15] Cyganik,P. , Szelagowska-Kunstman,K. , Terfort,A. , Zharnikov,M. , *Journal of physical chemistry C* 2008, *112*, 15466-15473.

[16] Cyganik,P. Buck,P, Strunskus,M, Shaporenko,T, Wilton-Ely J.D.E.T, Zharnikov, Wöll Ch. J. Am. Chem. Soc. (Article), 2006, 128, 13868-13878.